# Morphology of Poly(styrene-*block*-dimethylsiloxane) Copolymer Films

**Ningjing Wu,[1] Anna Zheng,[2] Yongmin Huang,[3] Honglai Liu[3]**

[1]*Key Laboratory for Rubber and Plastics Engineering of the Ministry of Education, Qingdao University of Science and Technology, Qingdao 266042, China*
[2]*Key Laboratory for Ultrafine Materials of the Ministry of Education, East China University of Science and Technology, Shanghai 200237, China*
[3]*State Key Laboratory of Chemical Engineering, East China University of Science and Technology, Shanghai 200237, China*

Received 15 July 2005; accepted 12 December 2005
DOI 10.1002/app.23952
Published online in Wiley InterScience (www.interscience.wiley.com).

**ABSTRACT:** The morphologies of poly(styrene-*block*-dimethylsiloxane) (PS-*b*-PDMS) copolymer thin films were analyzed via atomic force microscopy and transition electron microscopy (TEM). The asymmetric copolymer thin films spin-cast from toluene onto mica presented meshlike structures, which were different from the spherical structures from TEM measurements. The annealing temperature affected the surface morphology of the PS-*b*-PDMS copolymer thin films; the polydimethylsiloxane (PDMS) phases at the surface were increased when the annealing temperature was higher than the PDMS glass-transition temperature. The morphologies of the PS-*b*-PDMS copolymer thin films were different from solvent to solvent; for thin films spin-cast from toluene, the polystyrene (PS) phase appeared as pits in the PDMS matrix, whereas the thin films spin-cast from cyclohexane solutions exhibited an islandlike structure and small, separated PS phases as protrusions over the macroscopically flat surface. The microphase structure of the PS-*b*-PDMS copolymer thin films was also strongly influenced by the different substrates; for an asymmetric block copolymer thin film, the PDMS and PS phases on a silicon substrate presented a lamellar structure parallel to the surface at intervals. © 2007 Wiley Periodicals, Inc. J Appl Polym Sci 104: 1010–1018, 2007

**Key words:** atomic force microscopy (AFM); morphology; polysiloxanes; polystyrene

## INTRODUCTION

In recent years, thin films of block copolymers have received considerable attention because of their potential applications in self-assembly techniques. In these materials, two or more homopolymer chains are covalently bonded at their chain ends, and the interplay between the molecular connectivity among the different block chains and repulsive segmental interactions gives rise to a wide variety of microphase-separated morphologies with characteristic length scales of several tens of nanometers.[1–4] Control of the morphology in the films, including both the orientation and ordering of the copolymer microdomains, is essential for such applications. In general, the morphologies of thin copolymer films can be tuned by the molecular weight and composition of the diblock copolymer, the surface–block interactions, and the film thickness.[5,6]

A large number of studies have been reported on thermally equilibrated thin films of diblock and triblock copolymers, and they have revealed a rich variety of rather complex morphologies. Layers of microdomains, cylinders, or spheres oriented parallel to the interface in asymmetric block copolymer films have been reported.[7–12] Alexander et al.[9] studied thin and ultrathin islandlike morphologies, and the spacing could be controlled via the molecular weights of the different blocks of the respective copolymers. Fasolka et al.[11] cast ultrathin films of poly(styrene-*b*-*n*-butyl methacrylate) on miscut silicon waters and observed ordered morphologies along the corrugations of the substrate induced by thickness variations in the polymer films. Rockford et al.[12] deposited gold on miscut silicon wafers to produce alternating stripes of gold and silicon oxide with periods of 60 ± 10 nm, and the characteristic macroscopic ordering for the patterns of gold and silicon oxide was commensurate with the bulk lamellar period of the block copolymer.

The surface structure and morphology are important aspects of block copolymers, and they are determined by a minimization of the surface and interfacial energy. On chemically homogeneous surfaces, differences in the interfacial energy between the surface and the blocks of the copolymer generally induce different surface morphologies of the film to minimize the free energy. Much of the work[13–16] has been concentrated on lamella-forming diblock copoly-

*Correspondence to:* N. Wu (ningjing_wu@sina.com.cn or ninging_wu@yahoo.com.cn).

Journal of Applied Polymer Science, Vol. 104, 1010–1018 (2007)

**TABLE I**
**PS-*b*-PDMS Copolymer Characterization**

| Sample | PDMS molar fraction | $M_n \times 10^{-3}$ (GPC) | | | $M_w \times 10^{-3}$ | $M_w/M_n$ |
|---|---|---|---|---|---|---|
| | | Copolymer | PS block | PDMS block | | |
| 1 | 0.448 | 146.2 | 80.7 | 65.5 | 245.6 | 1.68 |
| 2 | 0.376 | 90.3 | 56.3 | 34.0 | 142.5 | 1.57 |
| 3 | 0.199 | 88.2 | 70.6 | 17.6 | 139.5 | 1.58 |
| 4 | 0.245 | 84.5 | 63.8 | 20.7 | 117.6 | 1.39 |
| 5 | 0.107 | 120.3 | 107.4 | 12.9 | 202.4 | 1.68 |

$M_n$ = number-average molecular weight; $M_w$ = weight-average molecular weight.

mers, in which the major effect lies in an alignment of the lamellae parallel to the confining surfaces. Fukunaga et al.[10] studied the thin-film structure of PS-*b*-Polystyrene-block-poly(2-vinylpyridine)-block-poly-(tert-butylmethacrylate) triblock copolymer (P2VP-*b*-PMMA) triblock copolymers on a polar substrate by both scanning force microscopy (SFM) and cross-sectional transition electron microscopy (TEM). The film exhibited a trapped, spongelike, microphase-separated structure covered by a thin, homogeneous layer of the lowest surface energy component on the free surface. In the region near the substrate, a thin, laterally inhomogeneous, microphase-separated layer was formed, which allowed the polar middle block to absorb at the polar substrate.

Over the last few years, poly(styrene-*block*-dimethylsiloxane) (PS-*b*-PDMS) copolymers have been studied for their potential technological importance as thermoplastic elastomers and as materials resistive to oxygen reactive-ion etching and for their unusual physical properties.[17–19] Although the morphology of PS-*b*-PDMS copolymers has been studied with TEM and small-angle X-ray scattering methods,[20–23] the surface morphologies of PS-*b*-PDMS copolymer thin films have been seldom systematically reported by atomic force microscopy (AFM) observation. In this work, we investigate the formation and morphology of immiscible PS-*b*-PDMS copolymer thin films. The variation of the polydimethylsiloxane (PDMS) ratio, annealing temperature, and solvents used for the coating deposition allowed the fabrication of films with different levels of heterogeneity and microstructure. Tapping-mode AFM and TEM measurements were used to characterize the morphology of the PS-*b*-PDMS diblock copolymer thin films.

## EXPERIMENTAL

### Preparation of the PS-*b*-PDMS copolymer

Styrene was obtained from Shanghai Jinshan Petrochemical Corp. (Shanghai, China). Hexamethylcyclotrisiloxane ($D_3$) was obtained from Xiamen Huaxin Chemical Co. (Shanghai, China). Cyclohexane, tetrahydrofuran (THF), and *N*,*N*-dimethylformamide (DMF) were provided by Shanghai Feida Industry Trade Corp., Ltd., Xia Men, China.

Styrene, washed with dilute sodium hydroxide to remove any inhibitors, was dried over calcium hydride and distilled under reduced pressure just before use. Cyclohexane, THF, and DMF were refluxed over sodium and distilled just before use. $D_3$ was dried over calcium hydride and freshly baked 4-Å molecular sieves. The *n*-BuLi initiator (1.0*M*) in cyclohexane was made with reference to the literature.[17]

The PS-*b*-PDMS copolymer was synthesized by the sequential anionic polymerization of styrene and $D_3$, which was carried out under argon in a reaction vessel equipped with a magnetic stirrer. Calculated amounts of cyclohexane, THF (cyclohexane/THF = 20/1 v/v), and styrene were introduced by the syringe technique into the reaction vessel. The *n*-BuLi initiator was added at room temperature, and red living polystyrene (PS) was obtained; the polymerization of styrene was carried out at this temperature for 0.5 h. Then, the $D_3$ monomer was slowly introduced as a solution in cyclohexane into a reaction vessel, and DMF was also added as a promoter. The temperature was increased to 60°C, and the red color disappeared by the transformation of the polystyryl active species into growing siloxanolate chains. After 4 h of stirring at this temperature, the reaction was stopped with ethanol as a terminating agent. After the removal of any unreacted $D_3$ with hexane, the homopolystyrene was removed by mixed solvents (cyclohexane/hexane = 25 : 1.2 w/w). After a purification procedure, the diblock samples were obtained in 90–98% yields.

The PDMS molar fractions, molecular weights, and molecular weight distributions of the block copolymers are summarized in Table I.

### Sample preparation

PS-*b*-PDMS copolymers were dissolved in toluene to make 0.01 g/mL solutions, and thin films were ob-

tained by the spin coating of a solution of the PS-*b*-PDMS copolymer in toluene at room temperature onto a freshly cleaved mica substrate or silicon substrate at 4000 rpm for 30 s, which had an atomically smooth surface. Films spin-coated from cyclohexane solutions of the PS-*b*-PDMS copolymer were prepared similarly from toluene solutions.

### AFM

The AFM topography images were obtained in the constant repulsive-force mode with an atomic force microscope (AJ-III, Aijian Nanotechnology, Inc., Shanghai, China) with a triangular microfabricated cantilever (Mikro Masch Co., MakroMasch, Russia) with a length of 100 μm, a Si tip with no coating, and a spring constant of 48 N/m. A resonance frequency in the range of 240–400 KHz was used; resonance peaks typically at 330 KHz in the frequency response of the cantilever were chosen for the tapping-mode oscillation. The AFM images were obtained with a maximum scan range of 20 × 20 $\mu m^2$; the scanning frequencies were usually in the range of 0.6–2.5 Hz/line. The measurements were carried out in air under normal conditions. All images presented in the article are height images.

### TEM

The films were prepared by the casting of one drop of a 1.0 wt % toluene solution of the diblock copolymer on a carbon-coated copper grid. The high electron density of the PDMS microphases in comparison with PS gave sufficient contrast without staining. The samples were examined with a JEM 1200EX2 (Hitachi Corp., Japan) transmission electron microscope operated at 120 kV. On the bright-field TEM pictures, the PDMS microdomains appeared black.

### Contact-angle measurements

The contact angles of water (pH 7) were measured at room temperature and ambient humidity with PC2000A contact measurement equipment (Shanghai Zhongchen Number Technology, Corp., Ltd., Shanghai, China). A Gilmont syringe with a blunt-tip needle was used to deliver water. To obtain relatively confident results, the water contact angle was measured in at least six different areas on the polymer film. Each of the reported contact angles was an average of at least 10 measurements taken within 20 s of each drop of water being applied, and the errors indicated a 95% confidence level. The samples were prepared in the same way as those subjected to AFM measurements. The water contact angle of the freshly cleaved mica substrate was 0°.

### Gel permeation chromatography (GPC) measurements

GPC, operated at 20°C with an America PE Co. GPC-200 with THF as the solvent at a flow rate of 1 mL/min, was used to measure the molecular weight and molecular weight distribution, with four columns packed with PS gel in series (the porosities were $2 \times 10^3$, $3 \times 10^4$, $2 \times 10^5$, and $8 \times 10^5$). The instrument was calibrated with narrow molecular weight distribution PS samples.

### $^1$H-NMR measurements

$^1$H-NMR spectra were recorded in deuterated chloroform at 500 MHz with an Bruker Avance, 500 spectrometer, Germany. The block ratios were calculated from $^1$H-NMR peak integrals.

## RESULTS AND DISCUSSION

In general, the morphology and composition of incompatible diblock copolymers can be influenced by many factors, such as the molecular weight, composition of the diblock copolymer, casting solvent, annealing temperature, film thickness, interfacial interactions, solvent evaporation, substrate pattern,[14] and electric fields.[24–26] This section is divided into four parts. First, we discuss the surface morphology of the copolymer thin films with different compositions. The second part includes discussions of the thermal annealing influence on the morphology of the copolymer films. Then, different solvents are used to investigate the effects of different solubility parameters on the film structure, and the effect of the polymer–substrate interaction on the film structure is discussed in the fourth section.

### Morphology of the spin-coated thin films of the PS–PDMS diblock copolymer

Ultradiluted solutions of the diblock copolymers in toluene were cast onto freshly cleaved mica and placed for 48 h to evaporate the solvents completely. In the spin-coating process, there are mainly three factors controlling the phase separation of copolymer films formed by quick evaporation of the solution: (1) different surface free energies, (2) different solubilities of the two polymers in the common solvent, and (3) polymer–substrate and polymer–air interactions. The final surface morphology structures of copolymer films are mainly dominated by a coeffect of the three factors.

Under the scanning condition used (i.e., the tapping mode), bright yellow represents a high place, whereas brown represents a low place in the AFM images. Figure 1 presents AFM height images show-

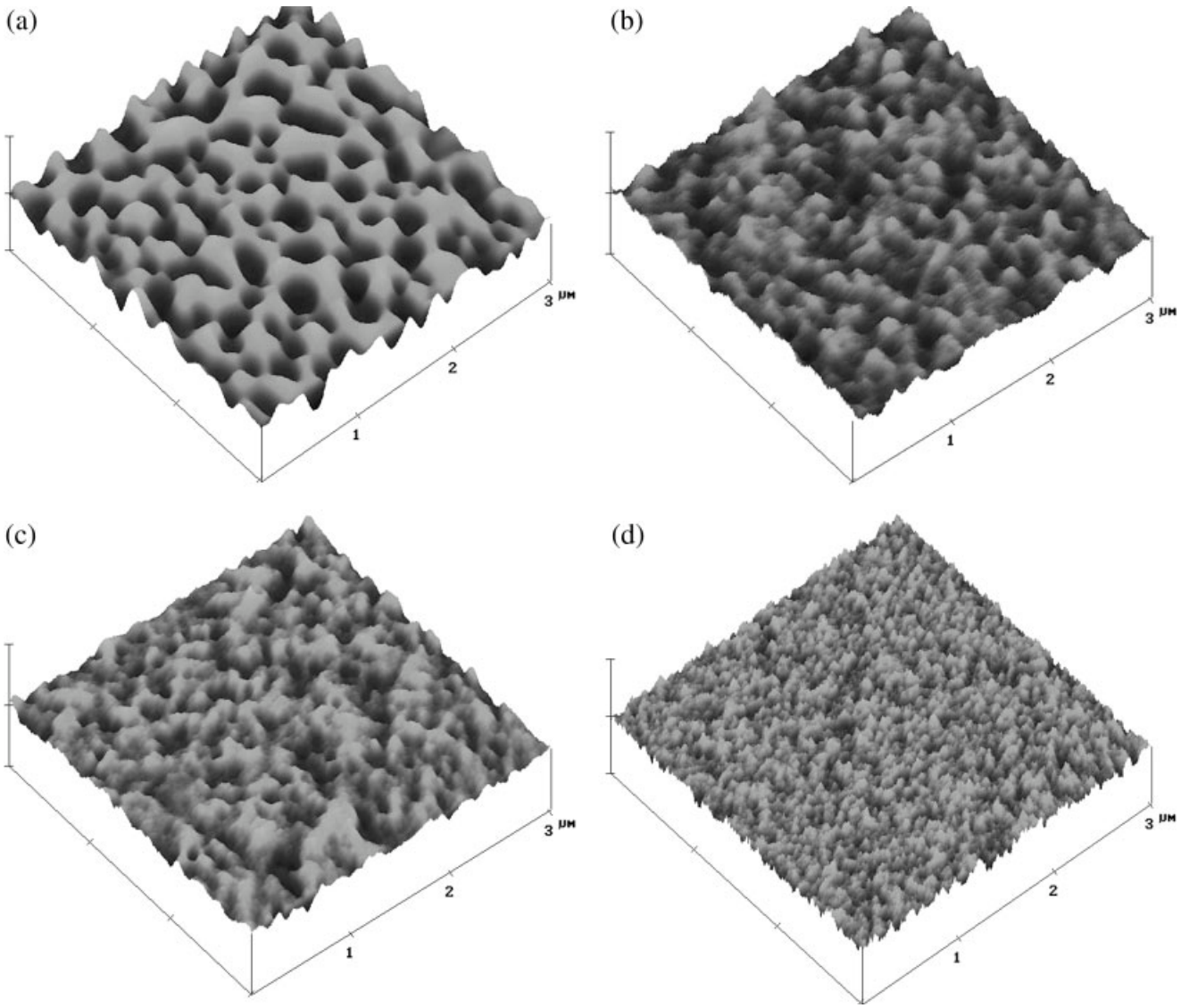


**Figure 1** AFM height images ($3 \times 3$ $\mu m^2$) showing the surface morphology of PS-*b*-PDMS copolymer films spin-cast onto mica from 0.01 g/mL solutions in toluene. The PDMS molar fractions were (a) 0.199, (b) 0.245, (c) 0.376, and (d) 0.448. The height scales are (a) 20, (b) 8, (c) 3, and (d) 3 nm.

ing the surface morphology for PS-*b*-PDMS copolymer films spin-cast onto mica. Two different phases exist in the AFM images, and phase separation occurred in all the copolymer films during the spin-coating process. Because their molecular weights were significantly different from one another, the domain size and shape of the dispersed and continuous phases also changed with the PDMS molar fraction of the PS-*b*-PDMS copolymer.

According to characteristic of the phase region in the AFM images, the experiments[6,14] proved that the phase exhibiting a lower solubility in the common solvent used for spin coating protruded over the other phase with the higher solubility in the copolymer. Because the phase of lower solubility first was deposited on the phase of higher solubility, whereas the phase of higher solubility was still dissolved in the same solvent, the other phase for the copolymer film was deposited on the mica after the solvent slowly volatilized, so solvent solubility played a decisive role in the morphology formation. Toluene, used as a common solvent in this spin-coating process, was a better solvent for the PS block than for the PDMS segments. Then, the PDMS phase deposited earlier than the PS phase and formed protrusions over the PS domains. While toluene slowly volatilized, the PS phase finally deposited onto the mica. Therefore, the yellow region represents the PDMS phase, whereas the brown region represents the PS phase. Because of the low surface energy of PDMS, PDMS tends to enrich to form a continuous phase on the surface, whereas PS has to be a dispersed phase. Figure 2 schematically shows the surface structure of the films spin-coated from tolu-

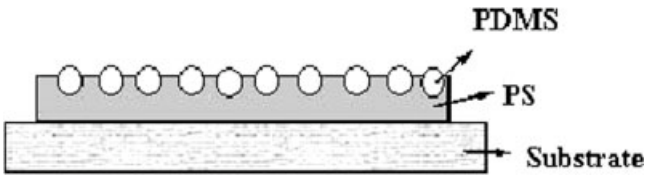


**Figure 2** Schematic representation of the surface phase-separated structure of the PS-*b*-PDMS copolymer thin films spin-cast from toluene solutions.

ene solutions of PS-*b*-PDMS diblock copolymers with different compositions.

Figure 1(a) presents AFM three-dimensional images corresponding to sample 3. From the pictures, we can clearly see a meshlike, microphase-separated structure. The PDMS continuous phase protruded on the PS dispersed phase as pits with a domain size of about 100 nm, and more PDMS phase was enriched on the surface with an increase in the PDMS content. As for the PS-*b*-PDMS copolymer thin film, the order of the magnitude of the surface free energy of PDMS ($21 \times 10^{-3}$ N/m)was lower than that of PS ($36 \times 10^{-3}$ N/m). Therefore, the PDMS segments tended to enrich on the surface to minimize the surface energies of the copolymer films; then for these films, increasing the PDMS content resulted in more PDMS phase protruding over the PS domains (Fig. 1b–d).

In other words, there are three factors affecting the phase-separated structures of copolymer films in this morphology formation process. First, PDMS has a lower surface energy than PS, so PDMS segments have a tendency to enrich on the surface to minimize the surface energy of the copolymer films; Second, the solubility of PS in toluene is better than that of PDMS, so the PDMS blocks form protrusions on the PS domains. Finally, the interaction between the PDMS blocks and mica substrate also affects the surface morphology. We discuss this in the following sections.

The bulk morphology of the PS-*b*-PDMS films was observed with TEM. Figure 3 presents electron photomicrographs of the thin films. The spherical structure was parallel to the surface, at which the PDMS blocks formed black, spherical microphases. These spheres were 20–40 nm in diameter, corresponding to different compositions. In these photographs, the blocks of PS are present in greater amounts and appear as a white, continuous phase. In Figure 3(a), the minimum width of the PS phase or the closest approach between the PDMS phases is about 60 nm. In comparison with AFM images [Fig. 1(a)], the morphological structure in the bulk [Fig. 3(a)] is largely different from that at the surface. PDMS blocks in the bulk appear as a dispersed phase, whereas PDMS blocks at the surface are a continuous phase. Because the AFM probe has a broadening effect, the dimensions obtained from AFM are often bigger than those from TEM measurements.

The contact angles of water were measured on the surfaces of the copolymer films. The results are shown in Figure 4. The contact angles of the PS and PDMS films were 89.5 and 112°, respectively. The contact angles of the copolymer films sharply increased with the PDMS molar fraction. The data clearly show that a top layer of the film on the surface had PDMS enrichment with an increasing PDMS fraction. With a lower PDMS content of the copolymer film, the PDMS

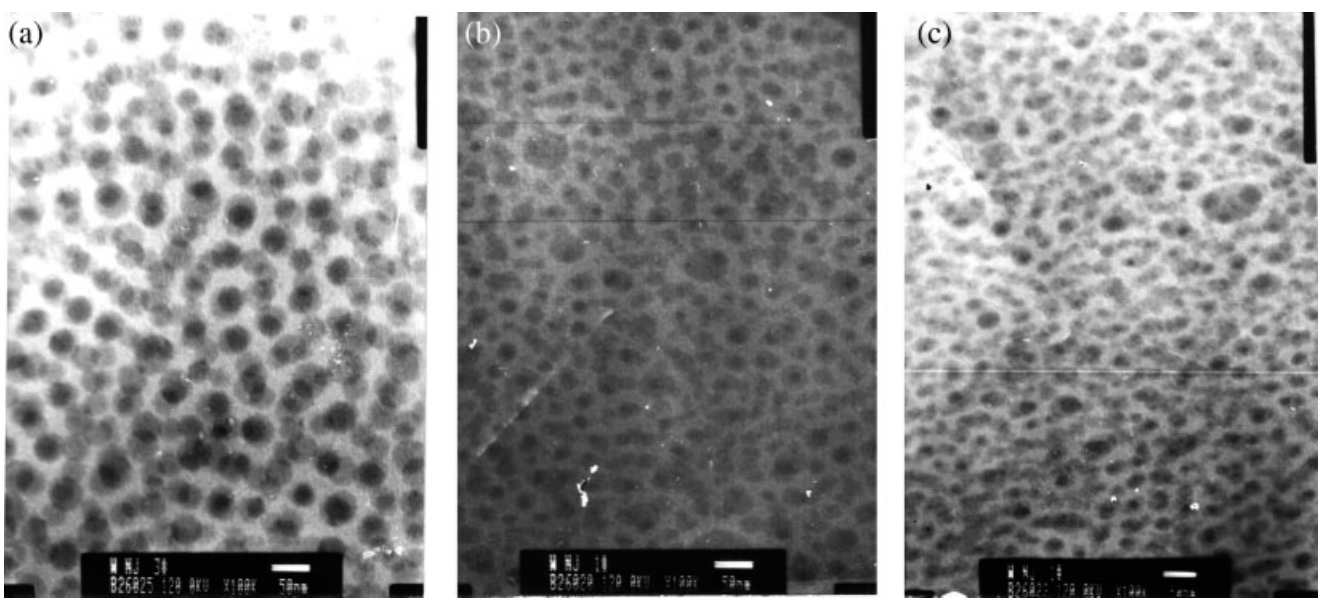


**Figure 3** TEM photographs of PS-*b*-PDMS copolymer films (multiple: 100 K, 50 nm). The PDMS molar fractions were (a) 0.199, (b) 0.245, and (c) 0.448.

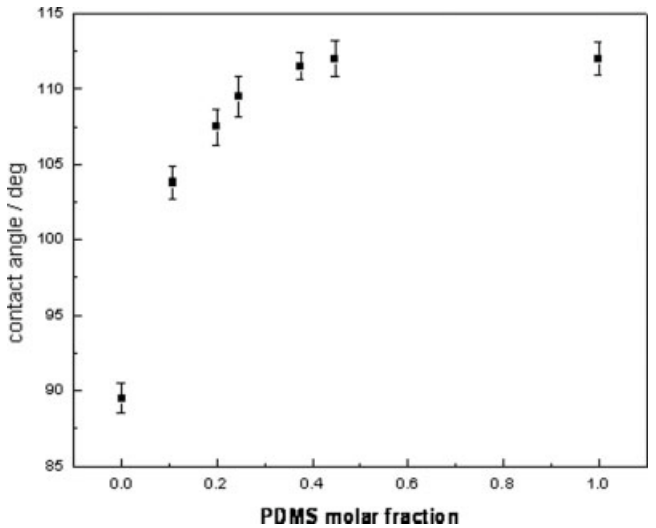


**Figure 4** Water contact angles of PS-*b*-PDMS films versus the PDMS molar fraction. The PDMS molar fractions of 0.0 and 1.0 represent pure PDMS and PS, respectively.

enrichment was strongly affected by the composition. When the PDMS fraction was close 50%, the top of the layer was almost completely occupied by PDMS because its contact angle almost equaled that of the pure PDMS layer, but there still were PS segments because of the interaction of PDMS and the mica substrate. Thus, the results corroborate the surface morphological structure of the PS-*b*-PDMS films from AFM measurements.

## Morphology of the annealed films

The annealing temperature effect on the morphology of block copolymer films has already been studied by some researchers.[20,27,28] In the following discussion, different thermal annealing is used to study the thermal equilibrium of the surface morphology of the PS-*b*-PDMS copolymer thin films.

A bicontinuous, spinodal-like morphology was observed for sample 2, as shown in Figure 5(a). The results from AFM experiments on unannealed thin films of the diblock copolymers showed poorly ordered morphologies. The poor ordering of the spin-casting sample was due to the short spinning process, during which the polymer chains did not have enough time to orient themselves to achieve good order.[16] Nevertheless, the domain spacings measured for the AFM data on these unannealed films are good indicators of the domain spacings in the equilibrium states. The PS microdomain size for the sample was about 100 ± 20 nm, larger than the TEM measurement result.

The surface structures of the films annealed at 80 and 120°C for about 36 h were studied, and their corresponding AFM height images are shown in Figure 5(b,c), respectively. An interesting phenomenon was observed for the annealed specimens with a lower PDMS fraction. Figure 5(b) shows that the PS and PDMS phase region remained the same, but the PDMS region appeared to be greater. Because the annealing temperature (80°C) was higher than the glass-transition temperature of PDMS (glass-transition temperature of PDMS = −123°C) and was lower than the order–disorder transition temperature of the PS block (glass-transition temperature of PS = 100°C),[20,28] the PDMS segments domains increased because of the movement of the PDMS segments at 80°C. When the sample was annealed at 120°C for 36 h, because the annealing temperature (120°C) was higher than the glass-transition temperature of either the PDMS or PS blocks, the immiscibility of the PDMS segments and PS blocks was higher than that of the specimens without thermal treatment; moreover, the PS block and PDMS block were still in a phase-segre-

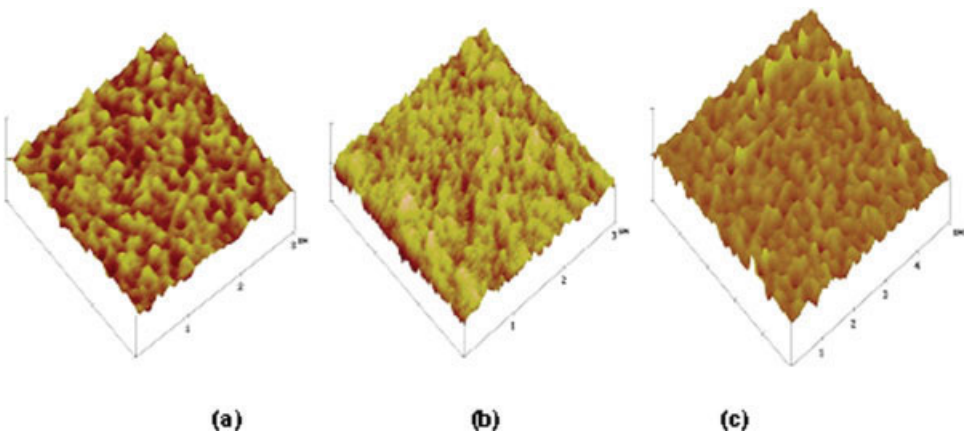


**Figure 5** AFM height images (5 × 5 μm$^2$) of PS-*b*-PDMS copolymer films spin-coated onto mica from 0.01 g/mL solutions in toluene: (a) before annealing at room temperature, (b) after annealing at 80°C, and (c) after annealing at 120°C. The height scales are (a) 8, (b) 5, and (c) 4 nm. [Color figure can be viewed in the online issue, which is available at www.interscience.wiley.com.]

**TABLE II**
**Solubility Parameter (δ) Values and Solvent Selectivity of the PS-*b*-PDMS Copolymer**

| Solvent/segment | δ [(cal/cm$^3$)$^{1/2}$] | CED (cal/cm$^3$)[a] | Solvent selectivity |
|---|---|---|---|
| Cyclohexane | 8.2 | 67.2 | PDMS |
| Toluene | 8.9 | 79.2 | PS |
| PDMS | 7.4 | 54 | — |
| PS | 9.1 | 83 | — |

[a] $\delta^2$.

gated state during the annealing. The immiscibility increased with the annealing temperature, so obvious microphase separation of the sample could also be observed [Fig. 5(c)]. The PS segments domains increased because of the movement of the PS segments at 120°C.

### Morphology of the films spin-cast from different solvents

The morphology of block copolymer films varies from solvent to solvent, as reported in the literature.[29,30] Solvent effects with different solubility and selectivity values on the surface morphology of copolymer films have seldom been studied. To investigate the effect of the casting solvent on the domain structure, cyclohexane was used to prepare the spin-coating solution. The solvent selectivity and the solubility parameters are shown in Table II. The solubility parameters of cyclohexane and PDMS were relatively close, so cyclohexane was a better solvent for PDMS blocks than PS blocks of the PS-*b*-PDMS diblock copolymer.

Figure 6 shows AFM topographical images of the PS-*b*-PDMS copolymer films spin-cast from toluene and cyclohexane solutions. The surface morphology of the copolymer thin film spin-cast from toluene was rich in the PDMS phase and poor in PS, which appeared as pits. However, for the thin film spin-coated from a cyclohexane solution, the morphology was different. The AFM image [see Fig. 6(b)] exhibits an islandlike surface structure having small protrusions separated by a characteristic spacing. The microdomain size of the protrusions was determined to be 100 ± 20 nm. For a direct comparison of AFM and TEM data, TEM images shown in Figure 3(c) obviously reflect the domain morphology found in the bulk of the thin film. The characteristic spacing of the PS phase was determined to be 40 ± 10 nm, which was less than that of the surface in the AFM images; the reason has already been explained.

The spherical morphology of the PS blocks as protrusions on the PDMS matrix formed an islandlike structure on a large scale. This is easy to understand because cyclohexane is a better solvent for PDMS than for PS and it selects PDMS segments only; therefore, PS deposits earlier than PDMS, and the PS phases form few protrusions on the PDMS domains. In addition, PDMS has a lower surface free energy than PS, so the PDMS phase has a higher affinity for the air–polymer surface to obtain a continuous state. The films spin-cast from toluene solutions, as previously described, had a contrast reverse because the solubility parameters of toluene and the PS block are rather close; on the other hand, PDMS, having less free energy than PS, tends to enrich at the surface, and PDMS has a higher affinity to bond with the silicone hydroxyl bond of the mica substrate than PS. These factors made the PDMS phase with protrusions form a rich phase on the PS phase.

### Morphology of the PS-*b*-PDMS copolymer films spin-coated onto different substrates

The substrate plays an important role in controlling the surface morphology of thin films. The substrate–segment interactions have been studied extensively for thin films of copolymers, including interplays and competitions and hence the parameters to control the morphologies.[30–37] There are long- and short-range interactions either between the air surface and the copolymer or between the substrate surface and the copolymers, giving rise to even richer unconfined thin films. Block-selective segregation at the substrate will occur when the wetting component

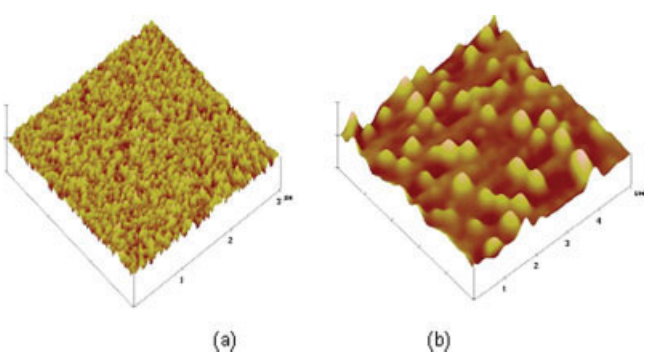


**Figure 6** AFM height images (3 × 3 μm$^2$) of PS-*b*-PDMS copolymer thin films spin-cast from different solvents: (a) toluene and (b) cyclohexane. The height scales are (a) 3 and (b) 20 nm. [Color figure can be viewed in the online issue, which is available at www.interscience.wiley.com.]

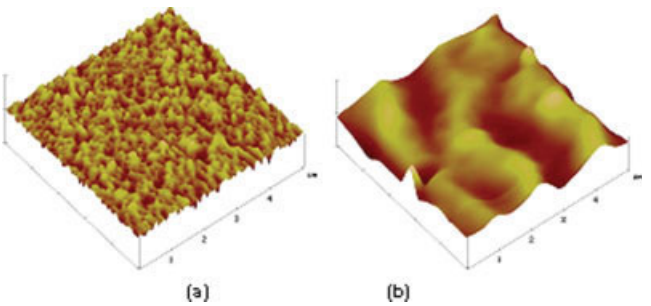


**Figure 7** AFM height image (5 × 5 μm$^2$) of PS-*b*-PDMS copolymer thin films spin-cast from toluene on different substrates: (a) mica and (b) silicon. [Color figure can be viewed in the online issue, which is available at www.interscience.wiley.com.]

provides the lowest interfacial tension or exhibits a specific affinity for the substrate. This results in so-called substrate-induced ordering. In this section, two types of substrates are used that have different interactions with PS and PDMS segments. The substrate dependence of the microphase-separated structure for the copolymer thin films is discussed.

Figure 7 presents AFM height images of the PS-*b*-PDMS copolymer thin films on the hydrophilic mica and hydrophobic silicone substrates. It is apparent that the shape and size of the copolymer thin film coated on the mica are very different from those of the film on the silicon substrate. The PDMS-rich domain of the film coated on the hydrophilic surface exhibits a wormlike morphology, whereas that coated on the silicon surface possesses parallel-like structure. The component surface fraction of the film coated on the surface is significantly different because the PS and PDMS blocks have different attractions for different substrates. The mica substrate contains silicon–hydroxyl bonds, which interact with dimethylsiloxane of PDMS blocks in the spin-casting process, and then the substrate–polymer interface affects the PDMS block enrichment and morphology on the surface; therefore, the PDMS blocks are distributed over the whole mica substrate. Although the silicon substrate has little interaction with PS blocks and PDMS blocks and PDMS segments have lower free energy than PS segments, PDMS segments are enriched at the air–polymer interface to minimize the air–polymer interfacial free energy. That is, at the air–polymer interface, there is a higher PDMS molar fraction than that in the bulk, and this makes it display a lamellar structure parallel to the surface.

In conclusion, this surface segregation in asymmetric block copolymers is believed to be governed by enthalpy factors and can be tuned to obtain a certain specificity for one block or both blocks. However, if the enthalpic driving force is absent, the surface segregation can be entropy-driven, and this results in surface segregation of the more flexible chain. Substrate-free block copolymer films allow the thin-film morphology with a noninteracting interface. The surface tension of the corresponding blocks will then induce preferential enrichment of the surface by the block with the lowest surface tension.

## CONCLUSIONS

Because PDMS segments have low surface energy, PDMS segments can be easily enriched at the surface of PS-*b*-PDMS copolymer thin films. For PS-*b*-PDMS copolymers with low PDMS concentrations, the AFM experimental results show that the surface morphology for PS-*b*-PDMS copolymer films spin-cast from toluene onto mica present a meshlike structure, which is different from the spherical structure in the bulk from TEM measurements. Obviously, there exists PDMS enrichment at the surface. The microdomain size and morphology at the surface change with the PDMS molecular weight and content of the PS-*b*-PDMS thin films.

The annealing temperature affects the surface morphology of PS-*b*-PDMS copolymer thin films. When the annealing temperature is lower than the glass-transition temperature of the PS block, the PDMS segment microdomains are increased because of the movement of the PDMS segments. Although the annealing temperature is higher than the glass-transition temperature of the PDMS and PS blocks, the immiscibility of different blocks increases, and this results in more obvious microphase separation at the surface morphology of the PS-*b*-PDMS copolymer thin films.

Because of the differences in the solubility parameters and solvent selectivity, the surface morphology is different from solvent to solvent. The surface morphology of copolymer thin films spin-cast from toluene is a wormlike structure, and the PS phase appears as pits in the PDMS matrix with a low PDMS fraction. However, for thin films spin-coated from cyclohexane solutions, an islandlike structure appears with a small, separated PS phase protruding over the macrosopically flat surface.

The microdomain morphology of thin copolymer films is also strongly influenced by the substrate. The differences in the interfacial energy between the different blocks at both the substrate surface and the free surface tend to align the resulting microdomain morphology of thin films. Generally, a preferential affinity of one of the blocks for an interface causes the block to prefer one interface. Unlike the mesh structure on a mica substrate, for an asymmetric block copolymer, the PDMS and PS phases of copolymer thin films on a silicon substrate surface present a lamellar structure parallel to the surface at intervals.

## References


1. Huang, E.; Russell, T. P.; Harrison, C.; Chaikin, P. M.; Register, R. A.; Hawker, C. J. Macromolecules 1998, 31, 7641.
2. Jeong, U.; Ryu, D. Y.; Kho, D. H.; Lee, D. H.; Kim, J. K.; Russell, T. P. Macromolecules 2003, 36, 3626.
3. Mackay, E. M.; Hong, Y.; Jeong, M.; Tande, M. B.; Wagner, J. N. Macromolecules 2002, 35, 8391.
4. Zhu, Y.; Gido, P. S.; Latrou, H.; Hadjichristidis, N. Macromolecules 2003, 36, 148.
5. Ho, R. M.; Chiang, Y. W. Macromolecules 2002, 35, 1299.
6. Elbs, H.; Fukunaga, K.; Stadler, R.; Sauer, G.; Magerle, R.; Krausch, G. Macromolecules 1999, 32, 1204.
7. Fasolka, J. M.; Banerjee, P.; Mayes, M. A. Macromolecules 2000, 33, 5702.
8. van Dijk, M. A.; van den Berg, R. Macromolecules 1995, 28, 6773.
9. Alexander, B.; Axel, H. E. M.; Georg, K. Macromolecules 2001, 34, 7477.
10. Fukunaga, K.; Hashimoto, T.; Elbs, H.; Krausch, G. Macromolecules 2002, 35, 4406.
11. Fasolka, M. J.; Harris, D. J.; Mayes, A. M.; Yoon, M.; Mochrie, S. G. J Phys Rev Lett 1997, 79, 3018.
12. Rockford, L.; Liu, Y.; Mansky, P.; Russel, T. P.; Yoon, M.; Mochris, S. G. J. Phys Rev Lett 1999, 82, 2602.
13. Lammertink, G. H. R.; Hempenius, A. M.; Vansco, J. G. Macromolecules 2001, 34, 942.
14. Peters, D. R.; Yang, M. X.; Nealey, F. P. Macromolecules 2002, 35, 1822.
15. Hahm, J.; Lopes, W. A.; Jaeger, H. M.; Sibener, S. J. J Chem Phys 1998, 109, 10111.
16. Corte, L.; Yamauchi, K.; Court, O. F.; Cloitre, M.; Hashimoto, T.; Leibler, L. Macromolecules 2003, 36, 7695.
17. Bajaj, P.; Varshney, S. K.; Misra, A. J Polym Sci Polym Chem Ed 1980, 18, 295.
18. Malhotra, S. L.; Bluhm, T. L.; Deslandes, Y. Eur Polym J 1986, 22, 391.
19. Zilliox, J. G.; Roovers, J. E. L.; Bywater, S. Macromolecules 1975, 8, 573.
20. Saam, J. C.; Fearon, F. W. G. Ind Eng Chem Prod Res Dev 1971, 10, 10.
21. Rosati, D.; Perrin, M.; Navard, P.; Harabagiu, V.; Pinteala, M.; Simionescu, B. C. Macromolecules 1998, 31, 4301.
22. Chu, J. H.; Rangarajan, P.; LaMonte Adams, J.; Register, R. A. Polymer 1995, 36, 1569.
23. Chen, X.; Gardella, J. A., Jr.; Kumler, L. P. Macromolecules 1992, 25, 6621.
24. Mansky, P.; DeRouchey, J.; Russell, T. P. Macromolecules 1998, 31, 4399.
25. Thurn-Albrecht, T.; De Rouchey, J.; Russell, T. P. Macromolecules 2002, 35, 8106.
26. Xiang, H.; Lin, Y.; Russell, T. P. Macromolecules 2004, 37, 5358.
27. Ritzenthaler, S.; Court, F.; Girard-Reydet, E.; Leibler, L.; Pascault, J. P. Macromolecules 2003, 36, 118.
28. Saam, J. C.; Gordon, D. J.; Lindsey, S. Macromolecules 1970, 3, 1.
29. Hu, F. Z.; Zheng, A.; Zhang, Q. The Surface and Interface of Polymer and Composite Material; Chinese Light Industry: Beijing, 2001
30. Buck, E.; Fuhrmann, J. Macromolecules 2001, 34, 2172.
31. Yang, X. M.; Peters, D.; Nealey, P. F. Macromolecules 2000, 33, 9575.
32. Yang, X. M.; Peters, R. D.; Nealey, P. F. Macromolecules 2002, 35, 2406.
33. Budkowski, A.; Bernasik, A.; Cyganik, P.; Raczkowska, J.; Penc, B.; Bergues, B.; Kowalski, K.; Rysz, J.; Janik, J. Macromolecules 2003, 36, 4060.
34. Kargupta, K.; Sharma, A. Langmuir 2003, 19, 5153.
35. Fukunaga, K.; Elbs, H.; Krausch, G. Langmuir 2000, 16, 3474.
36. Rockford, L.; Mochrie, S. G. J.; Russell, T. P. Macromolecules 2001, 34, 1487.
37. Fukunaga, K.; Hashimoto, T. Macromolecules 2003, 36, 2852.